European Journal of Medicinal Chemistry 44 (2009) 1921–1925

Contents lists available at ScienceDirect

European Journal of Medicinal Chemistry

journal homepage: http://www.elsevier.com/locate/ejmech

Original article

Novel *trans*-dichloridoplatinum(II) complexes with 3- and 4-acetylpyridine: Synthesis, characterization, DFT calculations and cytotoxicity

Gordana M. Rakić [a], Sanja Grgurić-Šipka [a,*], Goran N. Kaluđerović [b], Santiago Gómez-Ruiz [c], Snežana K. Bjelogrlić [d], Siniša S. Radulović [d], Živoslav Lj. Tešić [a]

[a] Faculty of Chemistry, University of Belgrade, Studentski trg 12-16, 11000 Belgrade, Serbia
[b] Department of Chemistry, Institute of Chemistry, Technology and Metallurgy, Studentski trg 14, 11000 Belgrade, Serbia
[c] Departamento de Química Inorgánica y Analítica, E.S.C.E.T., Universidad Rey Juan Carlos, 28933 Móstoles, Madrid, Spain
[d] Institute of Oncology and Radiology Serbia, Division for Experimental Oncology, Laboratory for Experimental Pharmacology, Pasterova 14, 11000 Belgrade, Serbia

ARTICLE INFO

Article history:
Received 4 September 2008
Received in revised form
11 November 2008
Accepted 11 November 2008
Available online 19 November 2008

Keywords:
Platinum(II)
Antitumoral activity
DFT
X-ray

ABSTRACT

Novel complexes of platinum(II) with 3- (**1**) or 4-acetylpyridine (**2**) have been synthesized and characterized by elemental analyses, IR, ^{1}H and ^{13}C NMR spectroscopy. Single crystal X-ray diffraction revealed the *trans* geometry of complex **2**. DFT calculations confirm formation of *trans* isomers for both complexes. The complexes have been tested for their cytotoxicity against HeLa (human cervical cancer), U2OS (human osteosarcoma), U2OScisR (human osteosarcoma cisplatin resistant), B16 (murine melanoma), MDA-453, MDA-361, and MCF-7 (human breast cancer), LS-174 (human colon cancer) and FemX (human melanoma) cell lines. The most promising compound *trans*-dichloridobis(4-acetylpyridine)platinum(II) (**2**) overcomes cisplatin resistance of U2OScisR cells after 48 h of drug exposure.

1. Introduction

Although cisplatin is the most used agent for the treatment of cancer, its efficiency against the malignancies is limited to a narrow range of tumors. There are several draw backs associated with cisplatin, including: toxicity and cross-resistance to the drug [1]. Therefore, enormous efforts are being made in the development of platinum complexes that would overcome these disadvantages [2–4]. Beside platinum(II), a large number of platinum(IV) complexes have been studied for potential anticancer properties [5–8]. Furthermore, ruthenium(II/III), titanium(IV) and recently tin(IV) complexes are also examined in *in vitro* antitumoral testings [9–13]. Among the thousands of cisplatin analogs, only a few drugs of the second and third generation alternatives, such as carboplatin, oxaliplatin and nedaplatin, improved the efficiency and clinical application [14–16]. On the other hand, transplatin showed less *in vitro* cytotoxicity and inactivity than cisplatin in *in vivo* tests [17]. For these reasons, investigations with transplatinum compounds were for a long time marginalized. Since the 1990s, many transplatinum complexes with *in vitro* growth inhibitory effects on different tumor cells were discovered [18,19]. The *in vitro* activity of these complexes has also been examined against cisplatin resistant cells [20–25]. New results concerning the cytotoxicity of transplatinum complexes confirm that there is virtually no structural barrier to obtain therapeutically active transplatinum complexes [26,27]. The most promising data has been obtained for transplatinum complexes containing heterocyclic, aliphatic, phosphoric or imino ether ligands. Complexes, *trans*-$[PtCl_2(L)_2]$ (L = pyridine, 4-methylpyridine) show reasonable *in vitro* antitumor activity against L1210 leukemia cells. This activity is greater than that of their *cis* counterparts [26]. In addition, the trinuclear platinum complex containing two monofunctional *trans*-$[PtCl(NH_3)_2]$ platinum units bridged by a platinum tetraamine unit *trans*-$[Pt(NH_3)_2(NH_2(CH_2)_6NH_2)_2]$ has entered clinical trials and is currently in phase II [28,29].

Prompted by *in vitro* activity of transplatinum complexes containing pyridine or 4-methylpyridine ligands, it was decided to synthesize *trans*-platinum(II) complexes with 3- or 4-acetylpyridine, *trans*-$[PtCl_2(n\text{-acetylpyridine})_2]$ ($n = 3$ or 4). The 3- and 4-acetyl derivatives of pyridine were chosen in order to investigate influence of the substituent position on the heterocyclic ligand in transplatinum complexes on the *in vitro* antitumoral activity. In addition, complex **2** was structurally analyzed by X-ray diffraction studies. The antiproliferative activity of the complexes **1** and **2** were tested on cancers from six different sources: human cervical cancer, human osteosarcoma, human osteosarcoma cisplatin resistant,

* Corresponding author. Tel.: +381 11 3336736; fax: +381 11 2184331.
E-mail address: sanjag@chem.bg.ac.yu (S. Grgurić-Šipka).

0223-5234/$ – see front matter © 2008 Elsevier Masson SAS. All rights reserved.
doi:10.1016/j.ejmech.2008.11.004

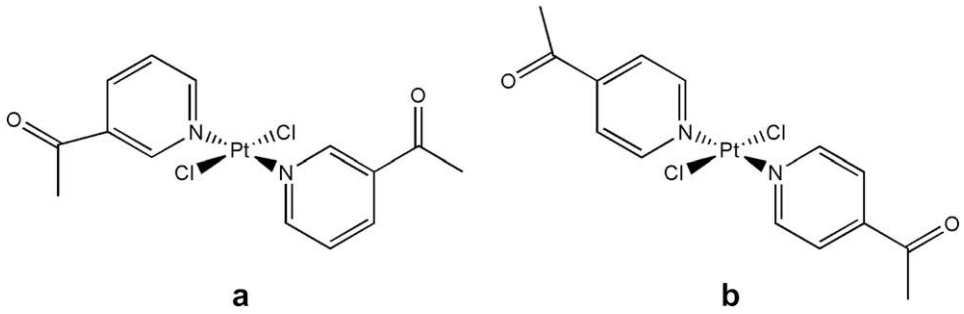

Fig. 1. (a) *trans*-[$PtCl_2$(3-acetylpyridine)$_2$] (**1**) and (b) *trans*-[$PtCl_2$(4-acetylpyridine)$_2$] (**2**) complexes.

murine and human melanoma, human breast cancer and human colon cancer by means of SRB assay.

2. Results and discussion

2.1. Chemistry

The complexes **1** and **2** were isolated as yellow microcrystalline solids in very high yield (87%) by the reaction of $K_2[PtCl_4]$ with the 3- or 4-acetylpyridine in 1:2 molar ratio in water. The structures of the complexes are presented in Fig. 1.

2.2. Spectroscopic measurements

The IR spectra of the free ligands were compared with those of the complexes to confirm their coordination to metal ion. In the IR spectra of the ligands and their corresponding complexes, it was observed that the $\nu_{(C=N)}$ vibration of the pyridine ring is shifted from 1583 to 1575 cm^{-1} in complex **1** and from 1594 cm^{-1} to 1555 cm^{-1} in complex **2** as a consequence of N-coordination of ligand to platinum ion. The bands related to the stretching vibrations of the carbonyl groups at 1690 cm^{-1} (3-acetylpyridine) and 1697 cm^{-1} (4-acetylpyridine) remained unchanged in the complexes. This fact is the evidence that these groups are not involved in the complex formation. The ^1H NMR spectrum of complex **1** shows signals at 9.39, 9.04, 8.46 and 7.65 ppm assigned to the pyridine protons, whereas for complex **2** these signals appear at 9.05 ppm and 7.86 ppm integrated as two hydrogens. Hydrogen atoms, *H*1 and *H*5, belonging to the pyridine ring, are noticeable shifted (**1**: $\Delta\delta = 0.30$ ppm; **2**: $\Delta\delta = 0.55$) to low field comparing with the spectra of the free ligands. The chemical induced shifts for the farther protons with respect to nitrogen atom (*H*3, *H*4, complex **1** and *H*2, *H*4, complex **2**) are twice less. This suggests that the binding of the ligand with the platinum ion in the complexes is realized through the nitrogen atom from the pyridine ring. The signal of the methyl group of the ligand appears at 2.63 ppm and at 2.51 ppm for complexes **1** and **2** respectively. Similarly in the ^{13}C NMR spectrum of complex **2** aromatic resonances at 154.39, 144.21 and 124.35 ppm (*C*1/*C*5, *C*3 and *C*2/*C*4, respectively) correspond to the resonances of a *para*-disubstituted aromatic ring, whereas for complex **1**, as expected, five chemical shifts at 156.67 (*C*5), 153.23 (*C*1), 138.59 (*C*3), 134.42 (*C*2) and 126.81 ppm (*C*4) appear in this region. Similarly to hydrogen atoms nearby nitrogen atom, the carbon atoms *C*1 and *C*5 are more downfield shifted in comparison with the free ligand since those are less shielded due to coordination of nitrogen to platinum ion.

2.3. X-ray study

The molecular structure of **2** is shown in Fig. 2 and selected bond distances and angles are listed in Table 1. In crystals of **2**, the molecules have the *anti* conformation with the acetyl groups on opposite sides of the platinum coordination plane. The Pt atom is located on a crystallographic centre of symmetry and shows square-planar coordination with Pt–N and Pt–Cl bond lengths of 2.005(5) and 2.301(2) Å respectively. The Pt–N and Pt–Cl distances are in the expected range for dichloridodi(pyridine)platinum(II) complexes [30]. Bond lengths and angles in the pyridine ring are as expected. The Cl–Pt–N angle of 90.1(1)° represents a value close to that expected in ideal square-planar coordination. The 4-acetylpyridine rings form angles of 49.7(5)° with the coordination plane. This dihedral angle is smaller than that found in similar compounds (56.2°, *trans*-[$PtCl_2(py)_2$]; 69.6(2)°/66.2(3)°, *trans*-[$PtCl_2$(3-picoline)$_2$]; 67.4(2)° *trans*-[$PtCl_2$(4-picoline)$_2$]) [30]. Packing forces seem to be important because the ligands are not sterically hindered near the coordination plane. Short atomic distances of 3.675(7) and 3.709(8) Å were found between C4···Cl1 and C7···Cl1 atoms, respectively.

2.4. Quantum chemical calculations

Two possible isomers of **1** and **2** (*cis* and *trans*) and for each isomer six (for **1**) and two (for **2**) possible conformers derived from the rotation of acetyl group bonded to pyridyl moiety were optimized. Among these possible isomers and their conformers we have selected the most stable *cis* and *trans* isomers, those having the lowest energy and thermodynamically the most stable form, as presented in Fig. 3. Calculations of their geometrical parameters

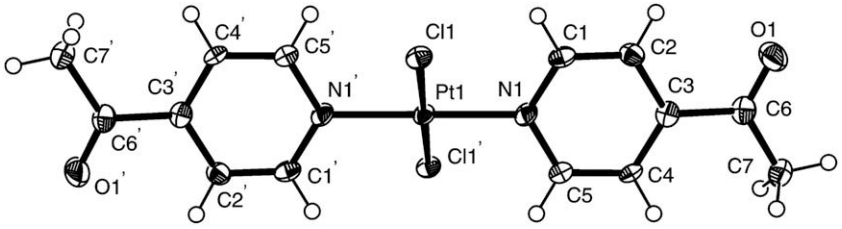

Fig. 2. ORTEP presentation of **2**. Displacement ellipsoids are plotted at the 50% probability level and H atoms are shown as small spheres of arbitrary radii.

Table 1
Selected bond lengths (Å) and angles (°) for complex **2**.

Bond lengths/Å		Bond angles/°	
Pt1–Cl1	2.301(2)	Cl1–Pt1–N1	90.1(2)
Pt1–N1	2.005(5)	Pt1–N1–C1	121.9(4)
O1–C6	1.21(1)	Pt1–N1–C5	120.1(4)
N1–C1	1.339(9)	N1–C1–C2	123.1(6)
N1–C5	1.364(8)	N1–C5–C4	121.2(6)
C3–C6	1.51(1)	O1–C6–C3	119.6(6)
C4–C5	1.38(1)	O1–C6–C7	121.5(6)

were performed by means of the DFT method, the B3LYP total energies calculated with SDD basis set. From DFT calculations it can be seen that the total energies obtained for **1** and **2** indicate the formation of *trans* geometrical isomers ($\Delta E_{(cis-trans)} = 12.2$ and 11.5 kcal/mol for **1** and **2**, respectively). Because the corresponding platinum(II) complexes were obtained from aqueous solution, Polarizable Continuum Model (PCM) with the dielectric constant of water was used for further calculations. As found in the gas phase and also here, calculations including solvent effects suggest that the *trans* isomer is the most stable isomer in both complexes ($\Delta E_{(cis-trans)} = 2.0$ and 2.1 kcal/mol for **1** and **2**, respectively). Data obtained in X-ray crystallography studies and DFT calculations for compound **2** are in very good agreement. DFT calculations for compound **1** indicate the formation of a *trans* isomer.

2.5. Cytotoxicity

The cytotoxicity of **1** and **2** were studied in nine malignant cell lines: HeLa (human cervical cancer), U2OS (human osteosarcoma), U2OScisR (human osteosarcoma cisplatin resistant), B16 (murine melanoma), MDA-453, MDA-361, and MCF-7 (human breast cancer), LS-174 (human colon cancer) and FemX (human melanoma), for both 48 and 72 h of incubation and were analyzed by dose-dependent curves and the IC_{50} (Table 2). Results revealed that both analogs showed antiproliferative activity against most of the investigated cell lines.

Among the most sensitive cells after 48 h of treatment, particularly with complex **2**, were platinum-resistant U2OScisR human osteosarcoma cells. The most resistant to both agents was LS-174 colon cancer cell line, as was expected. At 72 h, IC_{50}'s were not reached for either **1** or **2**, even though there were some activities achieved at 48 h for both.

Complex **2** was a 2–4 times more potent cytotoxic agent than complex **1**. The activity of **1** was higher after prolonged incubation in most of the cell lines except HeLa, U2OS, LS-174 and FemX. Contrary to this, cytotoxicity of the compound **2** remains similar or slightly higher after 72 h incubation in all cell lines, with the exception of cell line LS-174. The lowest IC_{50} concentrations were obtained with **2** in U2OScisR, U2OS, HeLa, B16, and FemX cells.

Looking at the activity after 48 h of incubation, **1** was found to be 2–9 times less potent compared to cisplatin. However after 48 h, **2** revealed comparable activity to cisplatin in HeLa cells and in U2OScisR cells and is even more potent than cisplatin in B16 melanoma. Furthermore, increasing the exposure time of cisplatin on the cell lines to 72 h leads to greater activity on HeLa and comparable with the activity of **2** on U2OScisR and B16 cell lines. This suggests compound **2** as more efficient after 48 h of action on cisplatin resistant U2OScisR and B16 melanoma cells.

From these investigations, the difference in activity between **1** and **2** may be attributed to the positioning of the acetyl substituent on the pyridine ligand. Overall it may be expected that greater activity can be observed for *trans*-dichloridoplatinum(II) complexes with substituents on the *para* (4) rather than the *meta* (3) position.

3. Conclusion

In this paper we report the synthesis, structural characterization and cytotoxicity of two new *trans*-dichloridoplatinum(II) complexes. These complexes were characterized by IR and NMR spectroscopy and elemental analysis. Complex **2** was also characterized by X-ray diffraction studies. The complexes showed moderated to potent antiproliferative activity on various cancer cell lines, with the exception of the LS-174 cell line. The position of the acetyl group on the pyridine ring was found to be the main reason for the difference in activity in almost all investigated cell lines. Complex **2** is able to overcome cisplatin resistance of human osteosarcoma cisplatin resistant cell line U2OScisR after 48 h of action. Further studies involving **2** currently in progress in our laboratory should reveal more detail on the mode of action on U2OScisR cell line.

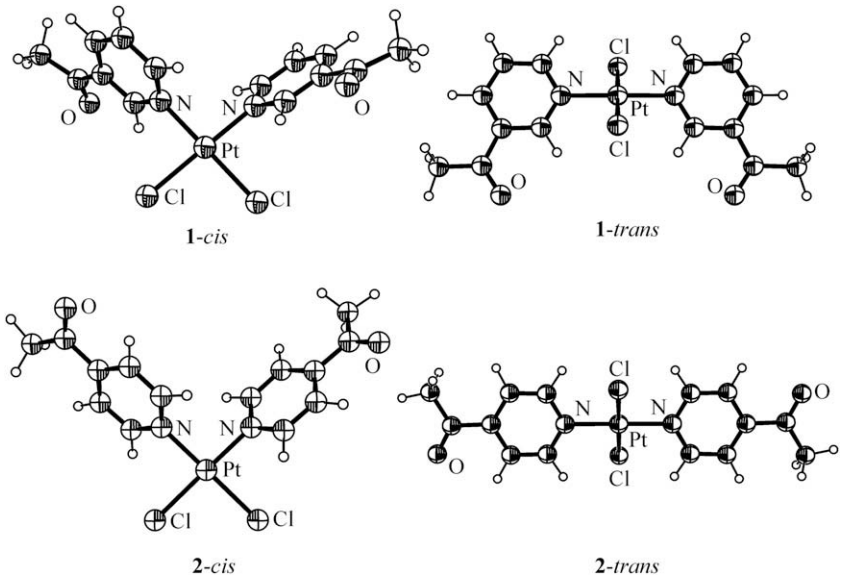

Fig. 3. The most stable *cis* and *trans* isomers of the calculated structures **1** and **2**.

Table 2
Cytotoxicity results expressed as IC_{50} values as determined from cell survival diagrams after 48 and 72 h treatments. The sign (>) indicates that IC_{50} value is not reached in the examined range of concentrations (the sign is in front of the maximum value of the concentration in the examined range of concentrations).

Cell lines	IC_{50} [μM]					
	1		**2**		Cisplatin	
	48 h	72 h	48 h	72 h	48 h	72 h
HeLa	27.8 ± 1.7	38.8 ± 4.2	7.3 ± 2.0	7.5 ± 0.9	6.9 ± 1.7	4 ± 0.5
U2OS	33 ± 4.4	32.7 ± 4.1	17.7 ± 3.2	8.8 ± 0.6	5.2 ± 0.6	4.0 ± 0.8
U2OScisR	25.1 ± 2.5	19.9 ± 3.8	9.2 ± 4.3	6.4 ± 0.9	12.2 ± 2.5	4.9 ± 1.0
B16	43 ± 5.1	14.5 ± 1.6	11.6 ± 3.7	9.4 ± 1.1	22.4 ± 0.4	12 ± 1.1
MDA-453	62.5 ± 10.1	17.7 ± 5.5	13.1 ± 4.8	11.5 ± 1.3	7.6 ± 0.7	5.7 ± 0.9
MDA-361	38.1 ± 4.7	11.5 ± 1.3	37.4 ± 9.8	25.1 ± 2.4	14.7 ± 1.2	25.9 ± 4.3
LS-174	53.9 ± 6.2	>100	36.2 ± 4.2	>100	9.7 ± 1.2	6.5 ± 1.3
MCF-7	27.3 ± 3.7	21.1 ± 4.9	13.3 ± 1.5	14 ± 1.3	3.4 ± 0.2	1.3 ± 0.6
FemX	20.2 ± 2.1	27.4 ± 5.5	9.7 ± 1.3	9.9 ± 1.2	2.1 ± 0.3	3 ± 0.2

4. Experimental

4.1. Materials and methods

3-Acetylpyridine and 4-acetylpyridine were commercially available and used without further purification. $K_2[PtCl_4]$ was prepared following the literature procedure [31].

Elemental analyses were carried out with Elemental Vario EL III microanalyser. Infrared spectra were recorded on a Perkin–Elmer FTIR 31725X spectrometer using KBr pellets (4000–400 cm^{-1}). The NMR spectra were recorded on a Varian Gemini 200 instrument. Chemical shifts for ^1H and ^{13}C spectra were referenced to residual ^1H and ^{13}C present in deuterated dimethylsulfoxide.

4.2. Chemical synthesis

4.2.1. Synthesis of trans-[$PtCl_2$(3-acetylpyridine)$_2$] (**1**)

To a solution of $K_2[PtCl_4]$ (0.19 g, 0.45 mmol) in water (5 mL) a solution of 3-acetylpyridine (0.10 mL 0.91 mmol) in water (3 mL) was added dropwise. The mixture was refluxed with stirring for 2 h. The pale-yellow product **1** was filtered, washed with ethanol and ether and dried. Yield: 0.20 g, 87%. m.p. 254 °C. Anal. calcd for $C_{16}H_{14}N_2O_2Cl_2Pt$: C, 33.08; H, 2.78; N, 5.51%. Found: C, 32.55; H, 3.04; N, 5.44%. ^1H NMR (199.97 MHz, DMSO-d_6, δ ppm): 9.39 (d, 1H, *H*1), 9.04 (d, 1H, *H*5), 8.46 (d, 1H, *H*3), 7.65 (t, 1H, *H*4), 2.63 (s, 3H, C*H*3). ^{13}C NMR (50.28 MHz, DMSO-d_6, δ ppm): 195.60 (*C*6), 156.67 (*C*5), 153.23 (*C*1), 138.59 (*C*3), 134.42 (*C*2), 126.81 (*C*4), 27.28 (*C*7). Selected IR (KBr, cm^{-1}): 1689 (s, C═O), 1575 (m, C═N), 1429, 1361, 1325 (pyridine ring).

4.2.2. Synthesis of trans-[$PtCl_2$(4-acetylpyridine)$_2$] (**2**)

To a solution of $K_2[PtCl_4]$ (0.19 g, 0.45 mmol) in water (5 mL) a solution of 4-acetylpyridine (0.10 mL 0.91 mmol) in water (3 mL) was added dropwise. The mixture was refluxed with stirring for 2 h. The pale-yellow product **2** was filtered, washed with ethanol and ether and dried. Yield: 0.20 g, 87%. m.p. 274 °C. Anal. calcd for $C_{16}H_{14}N_2O_2Cl_2Pt$: C, 33.08; H, 2.78; N, 5.51%. Found: C, 32.86; H, 2.93; N, 5.50%. ^1H NMR (199.97 MHz, DMSO-d_6, δ ppm): 9.05 (d, 2H, *H*1, *H*5), 7.86 (d, 2H, *H*2, *H*4), 2.51 (s, 3H, C*H*3). ^{13}C NMR (50.28 MHz, DMSO-d_6, δ ppm): 196.89 (*C*6), 154.39 (*C*1, *C*5), 144.21 (*C*3), 124.35 (*C*2, *C*4), 27.21 (*C*7). Selected IR (KBr, cm^{-1}): 1697 (s, C═O), 1555 (m, C═N), 1422, 1362, 1264 (pyridine ring).

4.3. X-ray crystallography of trans-[$PtCl_2$(4-acetylpyridine)$_2$] (**2**)

The data of complex **2** were collected with a CCD Oxford Xcalibur S (λ(Mo Kα) = 0.71073 Å) using multiscan mode. Semi-empirical absorption correction was carried out with SCALE3 ABSPACK [32]. The structure was solved with direct methods [33]. Structure refinement was carried out with SHELXL-97 [34]. However a relative high electron density residue remained close to Pt atom. The distance of Q1 to Pt and Q2 to Pt are *ca.* 8 and 7 pm, respectively. These peaks can be considered as spurious peaks of Pt due to its high electron density. All non-hydrogen atoms were refined anisotropically, and H atoms were placed at calculated positions and refined isotropically using the riding model. Table 3 lists crystallographic details.

Crystallographic data for the structural analyses of **2** have been deposited with the Cambridge Crystallographic Data Centre, CCDC-700683. Copies of this information may be obtained free of charge from The Director, CCDC, 12 Union Road, Cambridge CB2 1EZ, UK (fax: +44 1223 336033; e-mail: deposit@ccdc.cam.ac.uk or http//www.ccdc.cam.ac.uk).

Table 3
Crystallographic data for **2**.

Empirical formula	$C_{14}H_{14}Cl_2N_2O_2Pt$
Mr	508.25
Crystal system	Monoclinic
Space group	$P2_1/n$
a/Å	3.9021(2)
b/Å	24.368(1)
c/Å	8.0791(3)
$\alpha = \gamma$/°	90
β/°	102.408(4)
V/Å^3	750.26(7)
Z	2
D_{calc}/g cm^{-3}	2.250
M(Mo Kα)/mm^{-1}	9.711
F(000)	480
Θ Range/°	2.57–32.42
Refln. collected	21403
Refln. observed [$I > 2\sigma(I)$]	2303
Refln. independent	1645
Data/restraints/parameters	1303/0/98
Goodness-of-fit on F^2	1.14
*R*1, *wR*2 [$I > 2\sigma(I)$]	0.0578, 0.0977
*R*1, *wR*2 (all data)	0.0824, 0.1032
Largest diff. peak and hole/e Å^{-3}	3.08/−3.22

4.4. Computational details

Geometry optimizations were performed with the Gaussian 03 package [35]. All structures were optimized using the B3LYP functional [36]. The SDD basis set for all atoms was employed in the calculations [37]. All systems have been optimized without symmetry restrictions. The resulting geometries were characterized as equilibrium structures by the analysis of the force constants of normal vibrations. Polarizable Continuum Model (PCM) as implemented in Gaussian 03 was used for the prediction of solvent influence (water) on the complexes [35,38]. Supplementary data

associated with quantum chemical calculations can be obtained from the authors upon request.

4.5. Cytotoxicity assay

HeLa (human cervical cancer), U2OS (human osteosarcoma), U2OScisR (human osteosarcoma cisplatin resistant, kindly provided by Dr Paola Perego, Istituto Nacionale del Tumori, Milan, Italy), B16 (murine melanoma), MDA-453, MDA-361, and MCF-7 (human breast cancer), LS-174 (human colon cancer) and FemX (human melanoma) cell lines were maintained in RPMI1640 medium (Sigma–Aldrich, Cat. No. R7755), in a humidified atmosphere containing 5% (v/v) CO_2. The medium was supplemented with 10% heat-inactivated fetal bovine serum (Sigma–Aldrich, Cat. No. F4135), penicillin (100 units/ml), and streptomycin (100 μg/ml).

All cell lines were seeded at a density of 2500 cells/well in 96-well plates and left for 24 h to rest, before **1** and **2** were added. Preparation of test solutions was performed immediately before experiments by initially dissolving in DMSO to the stock concentration of 30 mmol/l and diluting further with the medium. Final concentrations achieved in treated wells for both **1** and **2** were 1, 3, 10, 30, and 100 μmol/l, with a maximum of 0.33% DMSO reached in wells with 100 μmol/l of **1** and **2**. Each concentration was tested in three triplicates on every cell line, and for both incubation periods. Cytotoxicity of **1** and **2** was evaluated after 48 and 72 h of incubation periods, using sulforodamine B (SRB, Sigma–Aldrich, Cat. No. S 1402-5G) colorimetric assay [39].

Dose-dependent curves, expressing the relationship between applied concentration and cytotoxicity, as well as IC_{50} concentrations (concentration of investigated drug that decreases the number of viable cells by 50% in treated cell population compared to non-treated control), were plotted by GraphPad Prism software.

Acknowledgements

Financial support by the Ministry of Science and Technological Developments (Project No's 142010, 142062, 145035) is gratefully acknowledged. We thank Mairéad E. Kelly (Martin-Luther-Universität Halle-Wittenberg, Halle, Germany) for helpful discussions.

References

[1] D. Wang, S.J. Lippard, Nat. Rev. Drug Discov. 4 (2005) 307–320.
[2] L. Kelland, Nat. Rev. Cancer 7 (2007) 573–584.
[3] G. Natile, M. Coluccia, Coord. Chem. Rev. 216–217 (2001) 383–410.
[4] N. Farrell, L.R. Kelland, in: N.P. Farrell (Ed.), Platinum-Based Drugs in Cancer Therapy, Humana Press, Totowa, 2000, pp. 321–338.
[5] S. Mijatović, D. Maksimović-Ivanić, J. Radović, D. Miljković, G.N. Kaluđerović, T.J. Sabo, V. Trajković, Cell. Mol. Life Sci. 62 (2005) 1275–1282.
[6] H.R. Mellor, S. Snelling, M.D. Hall, S. Modok, M. Jaffar, T.W. Hambley, R. Callaghan, Biochem. Pharmacol. 70 (2005) 1137–1146.
[7] M.D. Hall, T.W. Hambley, Coord. Chem. Rev. 1–2 (2002) 49–67.
[8] G.N. Kaluđerović, H. Schmidt, R. Paschke, B. Kalinowski, A. Dietrich, T. Mueller, D. Steinborn, J. Inorg. Biochem. 101 (2007) 543–549.
[9] S. Grgurić-Šipka, C.R. Kowol, S.-M. Valiahdi, R. Eichinger, M.A. Jakupec, A. Roller, Alexander, S. Shova, V.B. Arion, B.K. Keppler, Eur. J. Inorg. Chem. (2007) 2870–2878.
[10] M.A. Jakupec, M. Galanski, V.B. Arion, C.G. Hartinger, B.K. Keppler, Dalton Trans. (2008) 183–194.
[11] G. Kelter, N. Sweeney, K. Strohfeldt, H.-H. Fiebig, M. Tacke, Anti-Cancer Drugs 16 (2005) 1091–1098.
[12] S. Gómez-Ruiz, G.N. Kaluđerović, S. Prashar, D. Polo-Cerón, M. Fajardo, Ž. Žižak, T.J. Sabo, Z.D. Juranić, J. Inorg. Biochem. 102 (2008) 1558–1570.
[13] S. Gómez-Ruiz, G.N. Kaluđerović, S. Prashar, E. Hey-Hawkins, A. Erić, Ž. Žižak, Z. Juranić, J. Inorg. Biochem. 102 (2008) 2087–2096.
[14] P.J. O'Dwyer, J.P. Stevenson, S.W. Johnson, Drugs 59 (2000) 19–27.
[15] E. Cvitkovic, M. Bekradda, Semin. Oncol. 26 (1999) 647–662.
[16] J. Graham, M. Muhsin, P. Kirkpatrick, Nat. Rev. Drug Discov. 3 (2004) 11–12.
[17] K.M. Comess, C.E. Costello, S.J. Lippard, Biochemistry 29 (1990) 2102–2110.
[18] N. Farrell, T.T.B. Ha, J.P. Souchard, F.L. Wimmer, S. Cross, N.P. Johnson, J. Med. Soc. 32 (1989) 2240–2241.
[19] M. Leng, D. Locker, M.J. Giraud-Panis, A. Schwart, F.P. Initini, G. Natile, C. Pisano, A. Boccarelli, D. Giordano, M. Coluccia, Mol. Pharmacol. 58 (2000) 1525–1535.
[20] T.A. Connors, M.J. Cleare, K.R. Harrap, Cancer Treat. Rep. 63 (1979) 1499–1502.
[21] S. Radulović, Ž. Tešić, S. Manić, Curr. Med. Chem. 9 (2002) 1611–1618.
[22] S. Manić, Ž. Tešić, Z. Juranić, S. Radulović, M. Vrvić, B. Potkonjak, Z. Ilić, J. Exp. Clin. Cancer Res. 21 (2002) 519–526.
[23] S. Manić, Ž. Tešić, Z. Juranić, S. Radulović, J. BUON 6 (2001) 279–284.
[24] M.J. Lazic, K.K. Anđelković, D.M. Sladić, Ž.L. Tešić, S.S. Radulović, J. Exp. Clin. Cancer Res. 24 (2005) 63–68.
[25] N. Farrell, L.R. Kelland, J.D. Roberts, M. Van Beusichem, Cancer Res. 52 (1992) 5065–5072.
[26] U. Kalinowska-Lis, J. Ochocki, K. Matlawska-Wasowska, Coord. Chem. Rev. 252 (2008) 1328–1345.
[27] S. Arandjelović, Ž. Tešić, S. Radulović, Med. Chem. Rev. – Online 2 (2005) 415–422.
[28] N.J. Wheate, J.G. Collins, Coord. Chem. Rev. 241 (2003) 133–145.
[29] T. Servidei, C. Ferlini, A. Riccardi, D. Meco, G. Scambia, G. Segni, C. Manzotti, R. Riccardi, Eur. J. Cancer 37 (2001) 930–938.
[30] C. Tessier, F.D. Rochon, Inorg. Chim. Acta 295 (1999) 25–38.
[31] R.N. Keller, T. Moeller, J.V. Quagliano, Inorg. Synth. 2 (1963) 247–250.
[32] SCALE3 ABSPACK: Empirical absorption correction, CrysAlis – Software package, Oxford Diffraction Ltd., 2006.
[33] G.M. Sheldrick, SHELXS-97, Program for Crystal Structure Solution, Göttingen, 1997.
[34] G.M. Sheldrick, SHELXL-97, Program for the Refinement of Crystal Structures, Göttingen, 1997.
[35] M.J. Frisch, G.W. Trucks, H.B. Schlegel, G.E. Scuseria, M.A. Robb, J.R. Cheeseman, J.A. Montgomery Jr., T. Vreven, K.N. Kudin, J.C. Burant, J.M. Millam, S.S. Iyengar, J. Tomasi, V. Barone, B. Mennucci, M. Cossi, G. Scalmani, N. Rega, G.A. Petersson, H. Nakatsuji, M. Hada, M. Ehara, K. Toyota, R. Fukuda, J. Hasegawa, M. Ishida, T. Nakajima, Y. Honda, O. Kitao, H. Nakai, M. Klene, X. Li, J.E. Knox, H.P. Hratchian, J.B. Cross, V. Bakken, C. Adamo, J. Jaramillo, R. Gomperts, R.E. Stratmann, O. Yazyev, A.J. Austin, R. Cammi, C. Pomelli, J.W. Ochterski, P.Y. Ayala, K. Morokuma, G.A. Voth, P. Salvador, J.J. Dannenberg, V.G. Zakrzewski, S. Dapprich, A.D. Daniels, M.C. Strain, O. Farkas, D.K. Malick, A.D. Rabuck, K. Raghavachari, J.B. Foresman, J.V. Ortiz, Q. Cui, A.G. Baboul, S. Clifford, J. Cioslowski, B.B. Stefanov, G. Liu, A. Liashenko, P. Piskorz, I. Komaromi, R.L. Martin, D.J. Fox, T. Keith, M.A. Al-Laham, C.Y. Peng, A. Nanayakkara, M. Challacombe, P.M.W. Gill, B. Johnson, W. Chen, M.W. Wong, C. Gonzalez, GAUSSIAN 03, Revision C.02, Gaussian, J.A. Pople, Inc., Wallingford, CT, 2004.
[36] A.D. Becke, J. Chem. Phys. 98 (1993) 5648–5652;
C. Lee, W. Yang, R.G. Parr, Phys. Rev. B 37 (1988) 785–789;
S.H. Vosko, L. Wilk, M. Nusair, Can. J. Phys. 58 (1980) 1200–1211;
P.J. Stephens, F.J. Devlin, C.F. Chabalowski, M.J. Frisch, J. Phys. Chem. 98 (1994) 11623–11627.
[37] T.H. Dunning Jr., P.J. Hay, Modern Theoretical Chemistry, third ed., vol. 3, Plenum, New York, 1976, 1–28;
D. Andrae, U. Häußermann, M. Dolg, H. Stoll, H. Preuß, Theor. Chem. Acc. 77 (1990) 123–141.
[38] M. Cossi, G. Scalmani, N. Rega, V. Barone, J. Chem. Phys. 117 (2002) 43–54.
[39] P. Skehan, R. Storeng, D. Scudiero, A. Monks, J. McMahon, D. Vistica, J.T. Warren, H. Bokesch, S. Kenney, M.R. Boyd, J. Natl. Cancer Inst. 82 (1990) 1107–1112.